Cellulose Nanofibrils from Nonderivatizing Urea-Based Deep Eutectic Solvent Pretreatments

Panpan Li,[§] Juho Antti Sirviö,[§] Antti Haapala,[†] and Henrikki Liimatainen[§]*

[§]Fibre and Particle Engineering Research unit, University of Oulu, P. O. Box 4300, FI-90014 Oulu, Finland

[†]Wood Materials Science, University of Eastern Finland, P. O. Box 111, FI-80101 Joensuu, Finland

ABSTRACT: Deep eutectic solvents (DESs) are a fairly new class of green solvents applied in various fields. This study investigates urea-based DES systems as novel pretreatments for cellulose nanofibril production. In the experiments, deep eutectic systems having urea and ammonium thiocyanate or guanidine hydrochloride as a second component were formed at 100 °C and then applied to disintegrate wood-derived cellulose fibers. The DES-pretreated fibers were nanofibrillated into three different levels of mechanical treatments with a microfluidizer and their properties were analyzed. Moreover, nanofibril films were fabricated by solvent casting method. Both DES systems were able to loosen and swell the cellulose fiber structure as indicated by the increase in the lateral dimension of fibers. Nonpretreated birch cellulose fibers had difficulties in mechanical nanofibrillation as the clogging of thechamber occurred often. However, cellulose nanofibrils with widths ranging from 13.0 to 19.3 nm were successfully fabricated from DES-pretreated fibers with both systems. Translucent nanofibril films generated from DES-pretreated cellulose nanofibrils had good thermal stability and mechanical properties, with tensile strengths of approximately 135 −189 MPa and elastic modulus of 6.4−7.7 GPa. Consequently, both urea-based DESs showed a high potential as environmentally friendly solvents in the manufacture of cellulose nanofibrils.

KEYWORDS: cellulose nanofibrils; deep eutectic solvents; pretreatments; films; mechanical properties

INTRODUCTION

Deep eutectic solvents (DESs) consist of two or more interacting components, which result in a mixture of lower melting point compared with their individual precursor components.[1] The interaction is typically formed with hydrogen bonding.[2] DESs possess several superior properties in comparison to many traditional solvents:[3] they are easy to prepare, readily available with fairly low cost, biodegradable with relatively low−toxicity[4,5] and even recyclable.[6] Previously, DES systems have been investigated as one of the most promising alternatives for traditional solvents in various fields like metal electrodeposition,[7–9] material preparation,[10] solvent synthesis,[11–13] and lignocellulose pretreatment.[14,15] Recently, an efficient DES synthesis approach for choline chloride and urea was developed by using twin screw extrusion, which makes it possible to extend DES applications into industrial scale.[16]

Cellulose nanofibrils exist commonly in the cell wall of higher plants and are regarded as the nanoscale elementary units of cellulosic fibers. A single nanofibril consists of approximately 36 individual cellulose molecules each[17] which form a structure of 3−100 nm in diameter and several micrometers in length.[18] The cellulose nanofibrils have several attractive properties such as lightweight,[19] thermal stability, and very good mechanical properties.[20,21] These prerequisites make cellulose nanofibrils promising materials to apply, e.g., as reinforcement agents in paper and board,[22] biocomposites,[23,24] and packaging materials.[25] Nanofibrils are typically liberated under a high pressure mechanical disintegration.[26] Unfortunately, the mechanical fibrillation processes require a significant amount of energy and easily cause chamber clogging.[27] Thus, conventional reactive pretreatment methods such as chemical functionalization[28,29] or enzymatic treatment[30] are mostly applied to loosen the cellulose fiber structure and reduce the energy consumption of nanofibrillation. However, chemical reactive processes are costly and toxic, and enzymatic approaches are also expensive and time-consuming.[31,32] Therefore, DES systems as nonreactive, lesstoxic and inexpensive media lead to a sustainable pretreatment method in nanofibrillated cellulose (NFC)[33] and cellulose nanocrystals (CNCs) production.[34]

This work investigates the morphological, mechanical, and physical properties of NFCs derived from commercial birch pulp after pretreatments with different DES systems. Specifically, two urea -based DESs having ammonium thiocyanate or guanidine hydrochloride as a second component were compared and used as novel green pretreatments to promote nanofibrillation of wood cellulose fibers. The DES-pretreated cellulose fibers were nanofibrillated with three different levels of mechanical treatment using a microfluidizer and analyzed with transmission electron microscopy (TEM). The nanofibril films were cast from nanofibril suspensions and were characterized by scanning electron microscopy (SEM), thermogravimetric analysis (TGA), and a universal material testing machine.

EXPERIMENTAL SECTION

Materials. A Dry sheet of industrially bleached birch Kraft paper (Betula pendula) was oven-dried at 60 °C for 24 h, and used as a cellulose raw material. The properties of birch pulp were determined in a previous study.[35] Ammonium thiocyanate (NH_4SCN; ≥97.5%), guanidine hydrochloride ($NH_2C(NH)NH_2 \cdot HCl$; ≥99%) and urea (NH_2CONH_2; >99.0%) were from Sigma -Aldrich (Taufkirchen, Germany). Copper−ethylene diamine (CED) −solution was from FF-Chemicals (Oulu, Finland), and uranyl acetate dihydrate ($UO_2(CH_3COO)_2 \cdot 2H_2O$; 98%) was from Polysciences (Hirschberg an der Bergstasse, Germany). Deionized water was used in the whole experiment.

Cellulose Fiber Pretreatment in Deep Eutectic Solvent Systems. Two different DES systems, ammonium thiocyanate with urea, and guanidine hydrochloride with urea, were synthesized with the same molar ratio of 1:2 in a round-bottom flask. The DES mixtures (400 g) were heated at 100 °C in an oil-bath system until the mixtures become clear liquid. A 4.0 g of pulp was torn by hand into 1 cm *1 cm pieces, added into a DES and mixed continuously by magnetic stirring bar for 2 h at 100 °C. After the DES pretreatment, the flask was taken away from the oil-bath system and cooled for 10 min. Then, the DES-pretreated suspension was filtrated and washed by deionized water until the conductivity of the filtrate was below 20 μS cm^{-1}.

Fabrication of Cellulose Nanofibrils from Deep Eutectic Solvent Pretreated Cellulose Fibers. The DES-pretreated cellulose samples were diluted into aqueous suspensions (0.5%) which were first mixed at 11000 rpm with an Ultra-Turrax mixer (IKA T25, Staufen, Germany) for 1 min. Then, the suspensions were nanofibrillated into three different levels using a microfluidizer (Microfluidics M-110EH-30, Westwood, MA, USA). The fiber suspensions were first passed through a double-chamber system (400 and 200 μm) in a microfluidizer three times at a pressure of 1300 bar. At this point, one-third of the sample was collected (the first level of production, NFC I) and the remaining two-thirds of the sample was passed through 400 and 100 μm chambers an additional two times at a pressure of 2000 bar (the second level of production, NFC II). Similarly, half of the second level production was collected and the remaining pulp was passed through 200 and 87 μm chambers once at a pressure of 2000 bar (the third level of production, NFC III).

Preparation of Films from Deep Eutectic Solvent Treated Nanofibrils. The obtained nanofibril suspensions were degassed under vacuum and then fabricated into films (0.88 g of dry mass, 57.17 g m^{-2}) by solvent casting and dried under ambient conditions for 2 weeks.

Fiber Dimensions of Deep Eutectic Solvent Pretreated Cellulose. The DES-pretreated birch cellulose was diluted (0.008%) by deionized water. A 50 mL aliquot of well-mixed suspension was prepared and then analyzed by a Fiber Lab (Fiber Lab 2000, Metso Automation, Jyväskylä, Finland) image-based analyzer. The fibers were analyzed in terms of length (mm) and width (μm). The results obtained from the device for each treatment correspond to average values of over 5000 individual qualified fibers captured by scanning camera in the Fiber Lab instrument.

Degree of polymerization. The degree of polymerization (DP) values of DES-pretreated celluloses were obtained from the limiting viscosity values that were measured by dissolving the

cellulose pulp into cupriethylenediamine-solution (CED), according to the ISO 5351 standard. Samples were freeze-dried prior to the measurements. The DP was calculated according to[36]

$$DP = \left(\frac{(1.65[\,\eta\,] - 116H)}{C}\right)^{1.111} \quad (1)$$

where
[η] = the limiting viscosity [$dm^3\ kg^{-1}$],

C = the mass fraction of cellulose [74.8%],

H = the mass fraction of hemicellulose [24.7%]

The contribution from hemicellulose to the limiting viscosity value and the DP of cellulose pulp were taken into consideration, assuming that the average DP of hemicellulose is 140.[37]

Transmission Electron Microscopy. The morphological characteristics of the fabricated nanofibrils were analyzed by a Tecnai G2 Spirit transmission electron microscope (FEI Europe, Eindhoven, The Netherlands). Nanocellulose samples were highly diluted and well-distributed into a 10 mL plastic test tube. A tiny droplet (7 μL) of the dilution was dosed on the top of Butvar and carbon-coated copper grid. Specifically, the grid was precovered with polylysine[38] by applying a small droplet of 0.1% solution of polylysine on the top of the grid and allowing it to stand for 3 min. The excess polylysine was removed from the grid by touching the droplet with a corner of a filter paper. Then, the nanocellulose solution was placed on the top of the polylysine-covered grid and stable for 1 min. The excess of nanocellulose solution was wiped before addition of uranyl acetate (2% (w/v)) which was applied as negative a stain to cover the samples. Similarly, the excess amount of uranyl acetate was also removed with filter paper. The stained samples were dried at room temperature and later were analyzed at 100 kV under standard conditions. Images were taken by a Quemesa CCD camera. The widths of the individual nanocellulose fibrils as well as fibril aggregates were measured by iTEM image analysis software (Olympus Soft Imaging Solutions GMBH, Munster, Germany). Finally, over 100 well-distributed nanofibrils and nanofibril aggregates of each sample were measured. The final results were averaged, and the standard errors were calculated.

Field Emission Scanning Electron Microscopy. Nanofibril films were imaged by field emission scanning electron microscopy (FESEM, Zeiss Sigma HD VP, Oberkochen, Germany). The cross-sections were captured by snapping the frozen (liquid nitrogen) film strips. The tailored film sample was fixed to a carbon-coated carrier. An accelerating voltage at 1.00 kV as well as 2.00 kV was applied during imaging.

Thermogravimetric Analysis. Thermogravimetric analysis (TGA) of nanofibril films were carried out by a thermal analyzer (Netzsch STA 449F3 apparatus) under two separate atmospheres: the nitrogen flow and the air flow (dynamic air), at a constant rate of 60 mL min^{-1}. Approximate 5 mg of the room-temperature dried sample was carried by aluminum pan and was heated from 20

to 600 °C with a heating rate at 10 °C min^{-1}. The decomposition temperature (T_d) was taken when the temperature at the onset point of the weight loss in the TGA curve was obtained.

Tensile Test. The mechanical properties of the nanofibril films were measured with a universal material testing machine (Instron 5544, Norwood, MA, USA), equipped with a 100 N load cell. Films were always kept in a constant-temperature and-humidity condition (temperature and relative humidity were 23±1 °C and 50 ± 2%, respectively) during the sample preparation (films were cut into strips with a uniform width of 5 mm) and measurement processes. The thickness of each specimen was measured by a Precision thickness gauge (Hanatek, FT3, St. Leonards-on-Sea, U.K.) determining an average value of three random locations on the sample strip. For the tensile testing, a 40 mm gauge length was set under a manual prestrain of 0.05−0.1 N. The strain rate was controlled at 4 mm min^{-1}. After the stress − strain curve was plotted, the Young's modulus was calculated from the initial linear slope. The ultimate tensile strength was defined as the stress at the specimen breakage.

Statistical Analysis. Mechanical properties of nanofibril films were completed using values from more than seven qualified strips in each sample for tensile strength, maximum strain, and Young's modulus. Statistical evaluation of data was completed with using one-way analysis of variance (ANOVA), with (*) $p < 0.05$ suggesting significant difference.

RESULTS AND DISCUSSION

Characterization of DESPretreated birch fibers. In this study, DES based on urea together with ammonium thiocyanate (ATU) or guanidine hydrochloride (GHU) was studied as a pretreatment media prior the mechanical disintegration. Both components, ammonium thiocyanate and guanidine hydrochloride, formed clear liquid together with urea at 100 °C. The formation of ATU was observed to be faster compared to GHU and also the disintegration of cellulose fibers appeared to be faster in ATU than in GHU. For ATU, it took around 15 min to fully disintegrate cellulose into an even gel-like material, whereas for GHU it took approximately 30 min.

Both DES-pretreated birch fibers showed a clear increase in fiber width while the fiber length remained at almost the initial value with the untreated fibers (Table 1). The increase in lateral dimension of fibers indicated the fiber swelling and loosening of the fiber cell wall structure, likely due to DES influence on internal hydrogen bonding, and was more pronounced with the ATU than with GHU. The mass yields of fibers after DES pretreatments were 90% and 87% for ATU and GHU DESs, respectively, being similar to those obtained previously with choline chloride – urea (90%).[33] The yield decrease is most likely attributed to the dissolution of hemicelluloses.[39] Both DES systems had only a small effect on the degree of polymerization, showing approximately 5% reduction in DP compared to original cellulose fibers. These findings suggested that the used DES systems were able to swell and loosen the fiber macroscopic structural integrity without notable degradation of the molecular cellulose chain structure. This observation is in accordance with the notion that DES pretreatment facilitates the liberation of elemental structural units by fibrils by decaying hydrogen bonds between them, not by hydrolyzing the cell wall or in other ways deteriorating the fiber structure as with oxidation[28,29] or enzymatic treatments.[30]

Table 1. Width, Length, DP, and Yield of the Original Birch Fibers and after DES Pretreatment.

Sample	Width [μm]	Length [mm]	DP [-]	Yield [%]
ATU[1] fibers	18.40	0.84	3337	87
GHU[2] fibers	18.01	0.83	3315	90
Original fibers	17.80	0.85	3500	-

[1)] ATU = ammonium thiocyanate – urea DES, [2)] GHU = guanidine hydrochloride – urea DES

Nanofibrillation of DES Ppretreated Cellulose Fibers. The birch fibers pretreated by both DES systems passed through the microfluidizer chambers smoothly without blockages, while the disintegration of untreated fibers was not possible due to severe chamber plugging. The obtained aqueous nanofibril suspensions were gel-like and slightly turbid already after the first level of treatment (NFC I) and became more viscous after further passes through the microfluidizer (NFC II and NFC III) (Figure 1).

Figure 1. Ammonium thiocyanate – urea pretreated nanocellulose suspension in three different levels of mechanical disintegration.

The TEM images confirmed that both ATU and GHU DES systems benefited birch fibers mechanical disintegration into nanofibrils. Generally, the lateral dimension in samples varied from 13.0 to 19.3 nm (Table 2), indicating that the samples contained individual nanofibrils but also larger aggregates. Previously, nanofibril aggregates of width 25 ± 6 nm were produced through sequential periodate-chlorite oxidation.[29] In addition, enzyme-pretreated NFC with a large variation in diameter from 20 to 650 nm has also been reported.[40] Here, also individual nanofibrils with a width of 3–5 nm were detected easily in all levels of nanofibrillation (I-III) with both DES-pretreated cellulose fibers. The widths of the individual nanofibrils were comparable to those obtainable with TEMPO and periodate-chlorite oxidization methods. [41–43]

Table 2. Width of the Cellulose Nanofibrils Obtained after Different DES Pretreatments (ATU and GHU).

	ATU			GHU		
Samples	NFC I	NFC II	NFC III	NFC I	NFC II	NFC III
Width (nm)	19.3±21.4	13.1±10.7	16.6±15.2	13.0±11.8	15.8±11.5	15.2±14.7

The individual, well-dispersed nanofibrils and small nanofibril bundles can be noticed in Figure 2 (images B and C′). Larger nanofibril bundles with widths around 100 nm appeared in the samples

treated with the first level of nanofibrillation (NFC I), such as in images A and A´ (Figure 2). Moreover, there were still some larger fragments of fiber cell walls observed with all three levels of mechanical disintegration (image C in Figure 2).

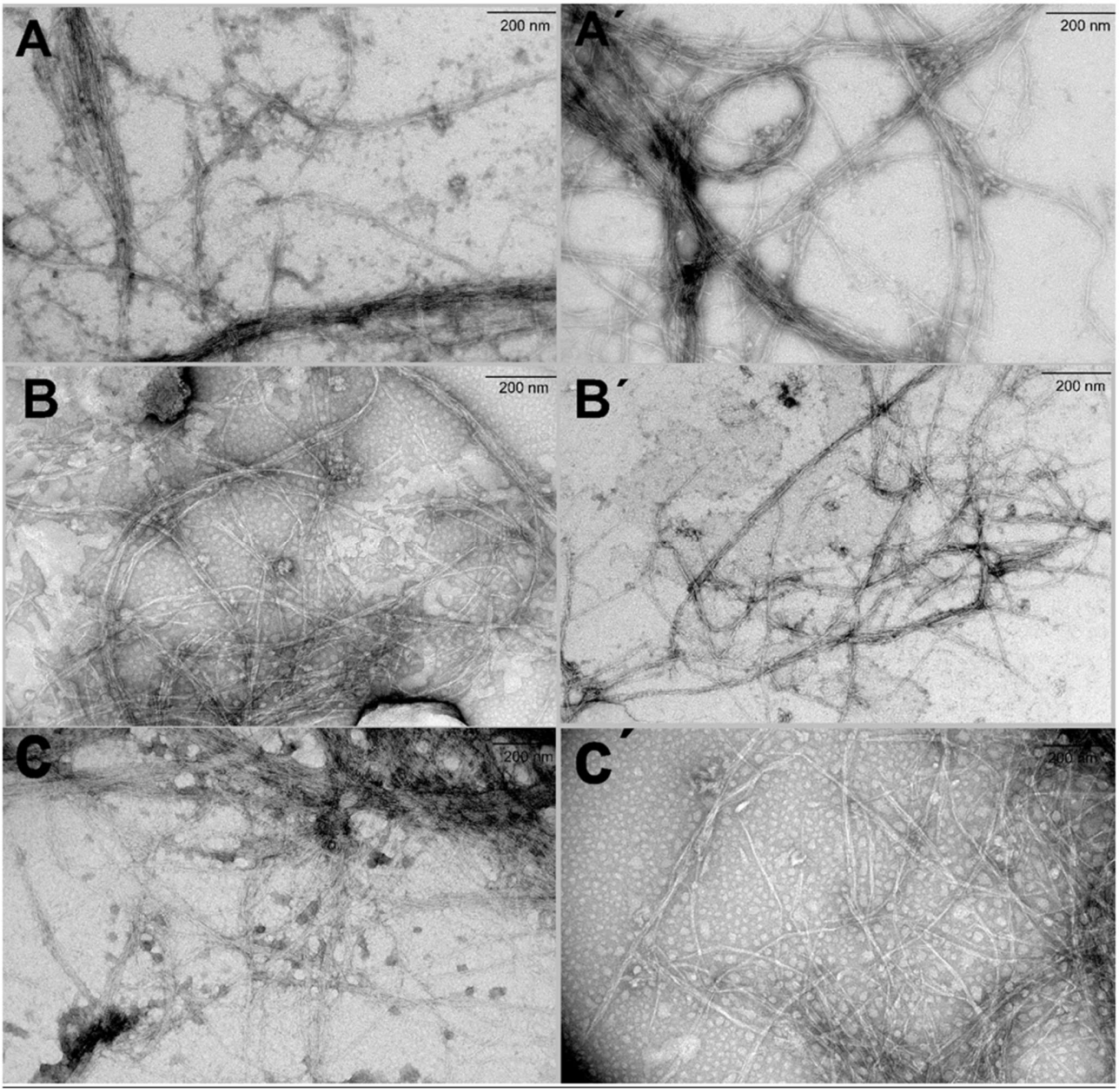

Figure 2. TEM images of nanofibrils produced from DES-pretreated birch fibers in different levels of nanofibrillation (NFC I – III): ATU-NFC I (A), ATU-NFC II (B), ATU-NFC III (C), GHU-NFC I (A´) GHU-NFC II (B´) and GHU-NFC III (C´).

Structure of Nanofibril Films. The films were generated from the obtained nanofibrils using a solvent casting method. All the film samples were translucent (Figure 3). It was difficult to identify the difference between ATU and GHU DES-pretreated nanofibril films from their appearance. FESEM imaging was required to study the surface morphology of these films. The surfaces of films were gradually smoother with increased severity of mechanical treatment for both DES-pretreated nanofibrils (Figure 4). The films generated from the first level of nanofibrillation contained some distinctly larger particles (A and A′, Figure 4), which likely consisted of bundles of individual nanofibrils and larger cell wall fragments.

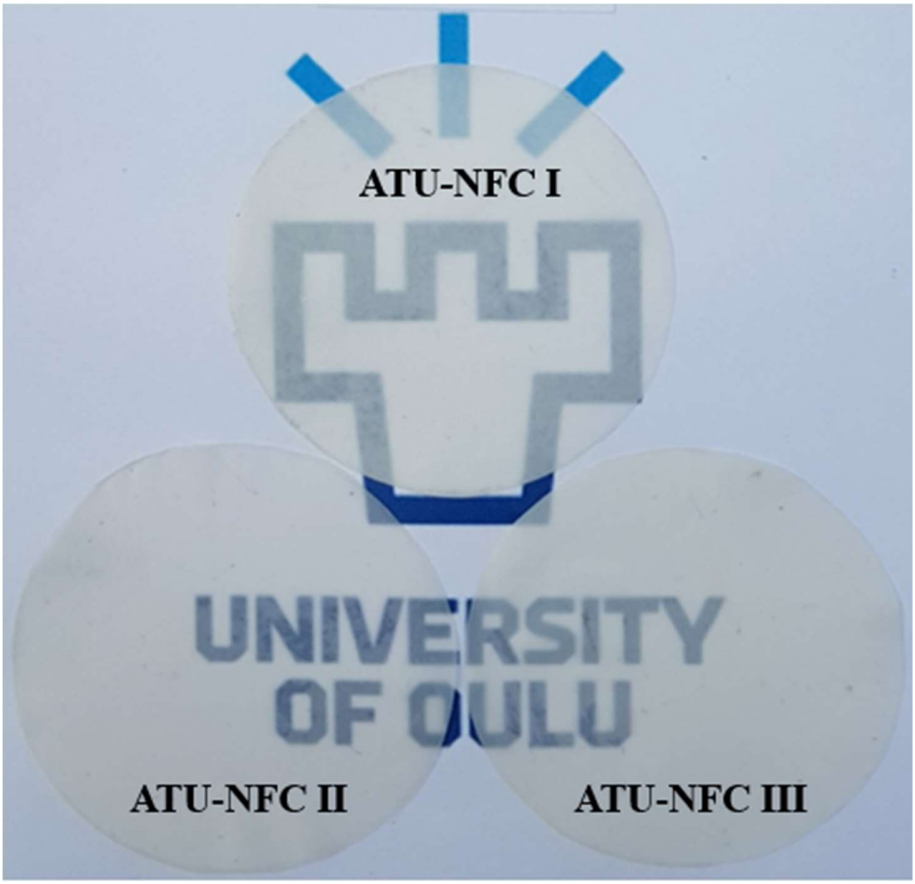

Figure 3. Nanofibril films made from ammonium thiocyanate – urea pretreated cellulose fiber, mechanical disintegration in three different levels.

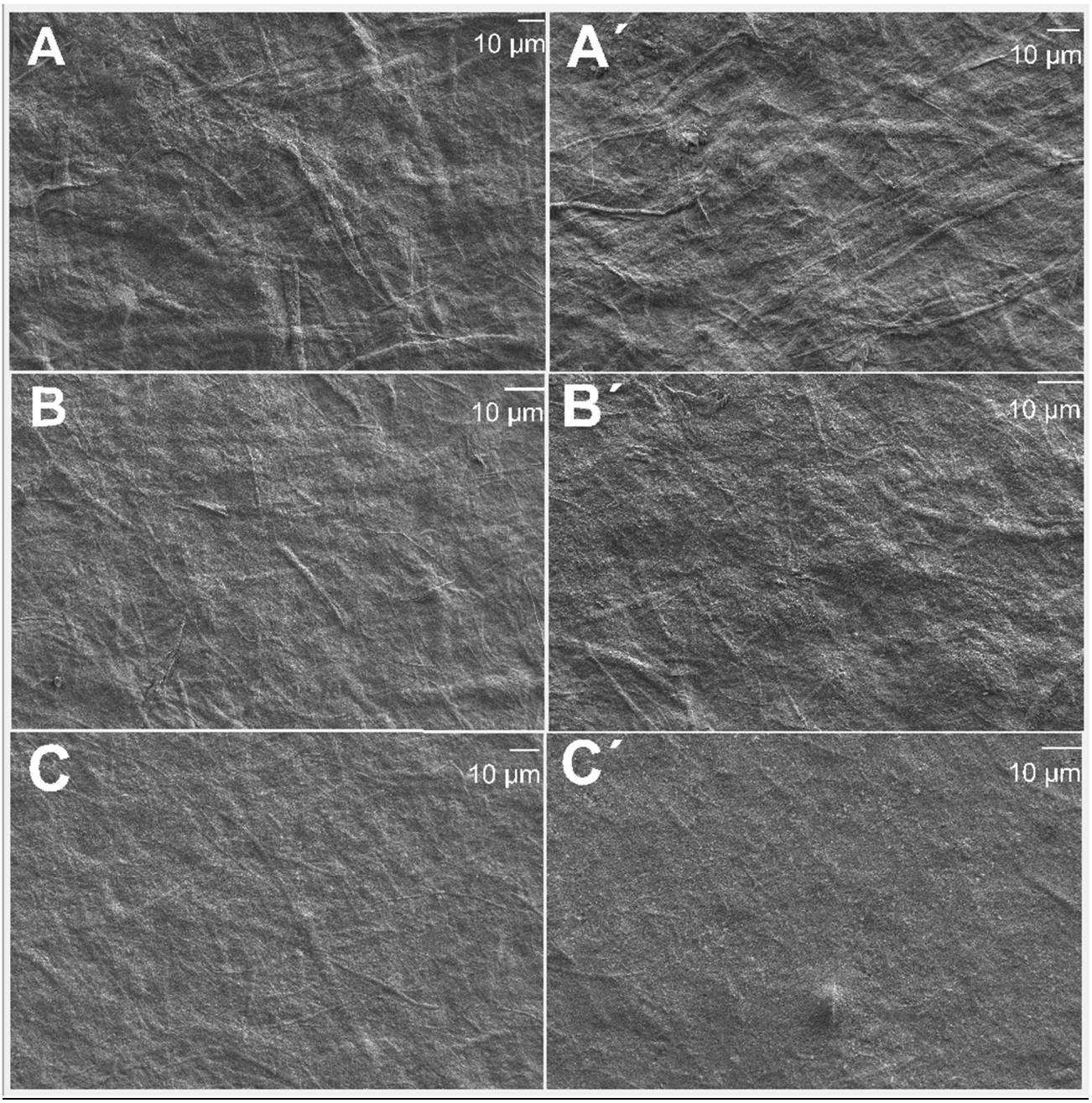

Figure 4. Surface FESEM images (x500 magnification) of nanofibril films generated from DES-pretreated birch cellulose using different levels of nanofibrillation (NFC I – III): ATU-NFC I (A), ATU-NFC II (B), ATU-NFC III (C), GHU-NFC I (A´), GHU-NFC II (B´), and GHU-NFC III (C´).

Even though fibers seemed to become evenly disintegrated to nanofibrils in the mechanical nanofibrillation processes, some unexpected white flakes that may originate from the impurities during the disintegration and/or film forming showed up in both DES nanofibril films. Compared

with ATU-NFC III, not only more white flakes but also clearer porous regions were observed in the films of GHU-NFC III (Figure 5). The cause of the porous regions is unknown.

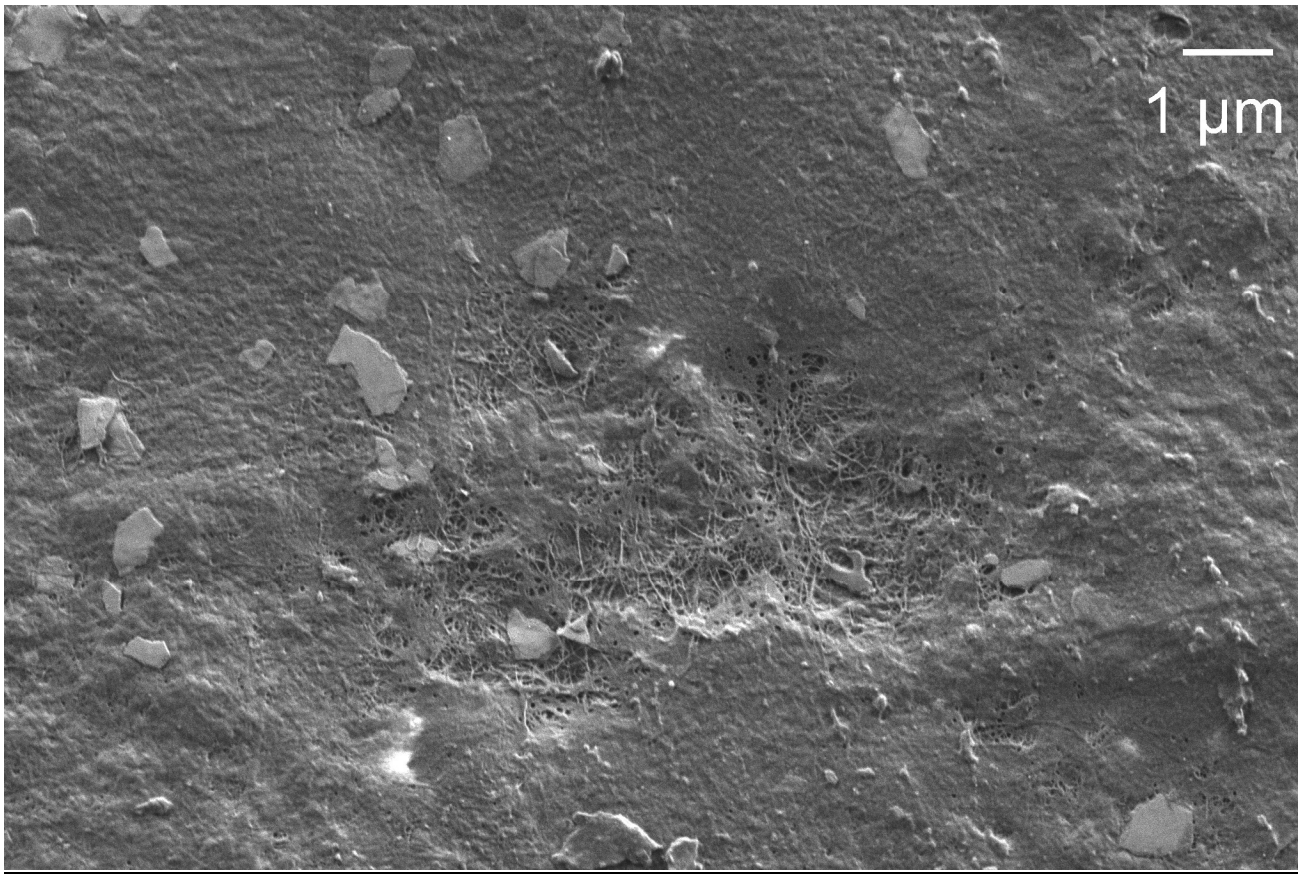

Figure 5. FESEM image of the nanofibril film surface generated from GHU-NFC III: white flakes and porous regions.

The cross-sectional FESEM images of the nanofibril films showed clearly the layered structures of the films (Figure 6). The cross-section of the films became smoother, and the layered structure was gradually faded away with the increased mechanical disintegration (images A, B and C in Figure 6).

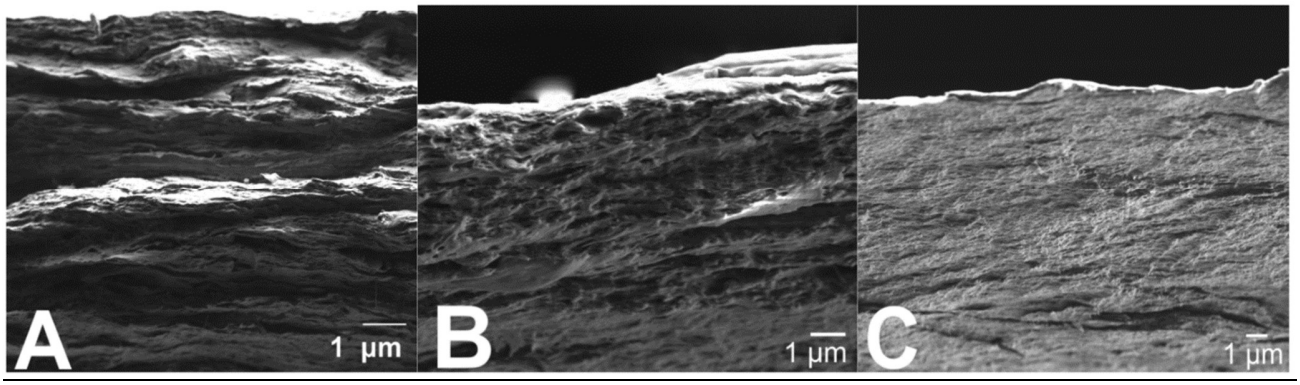

Figure 6. FESEM images of the nanofibril film cross-sections, obtained from DES-pretreated birch pulp: GHU-NFC I (A), GHU-NFC II (B), and GHU-NFC III (C).

Thermal Stability of Nanofibril Films in the Air and N_2. The thermal behaviors of the nanofibril films were analyzed by TGA at both air and N_2 atmosphere. Nonfibrillated, original birch fibers with and without DES pretreatment were used as reference samples.

The TGA curves indicate the processes of cellulose degradation. Generally, a bimodal weight loss curve occurred in every sample at air atmosphere (images A and B in Figure 7). In the first stage, when the temperatures were below 100 °C, all of the samples had low weight loss because of the evaporation of water. No cellulose degradation occurred at this stage.[44] The original birch fibers and nanofibril films started a similar degradation approximately at the temperature of 250 °C. However, the DES-pretreated birch fibers showed better thermal stability with a higher initial degradation temperature at ca. 270 °C, which may be due to the removal of hemicelluloses by DESs.[45,46] For the nanofibers, the decreased DP by mechanical disintegration is likely responsible for a lower thermal stability than DES-pretreated fibers.[47,48]

The major weight loss of the original birch fibers with and without DES treatment takes place between 270 °C (250 °C for non-DES-pretreated pulp) and 320 °C, and the residual weight after this stage was ca. 20%, whereas there is still ca. 38% nanofibril residual after the films dramatically degraded at the temperature range from 250 to 325 °C. Furthermore, the degradation rate of nanofibrils was significantly lower than both DES-pretreated fibers and original birch fibers (images B and B′ in figure 7). This may be due to a more efficient hydrogen bonding among nanofibrils. In addition, the temperature of maximum weight loss rate for birch fibers is slightly lower when compared with DES-pretreated fibers and nanofibers (can be seen from the first derivate curve). Finally, at the end of the second stage, nanofibers had a slightly higher temperature (440–470 °C) than birch fibers with and without DES pretreatment (420–440 °C).

At N_2 atmosphere, samples had similar behavior but with monomodal degradation curves compared to air (image A′ and B′ in Figure 7). No matter whether in the air or in N_2, DES-pretreated samples exhibited better initial degradation temperature than original birch fibers,

indicating that DESs as a pretreatment method leads to an enhanced thermal stability of cellulose fibers, which may be associated with hemicellulose dissolution into DES.

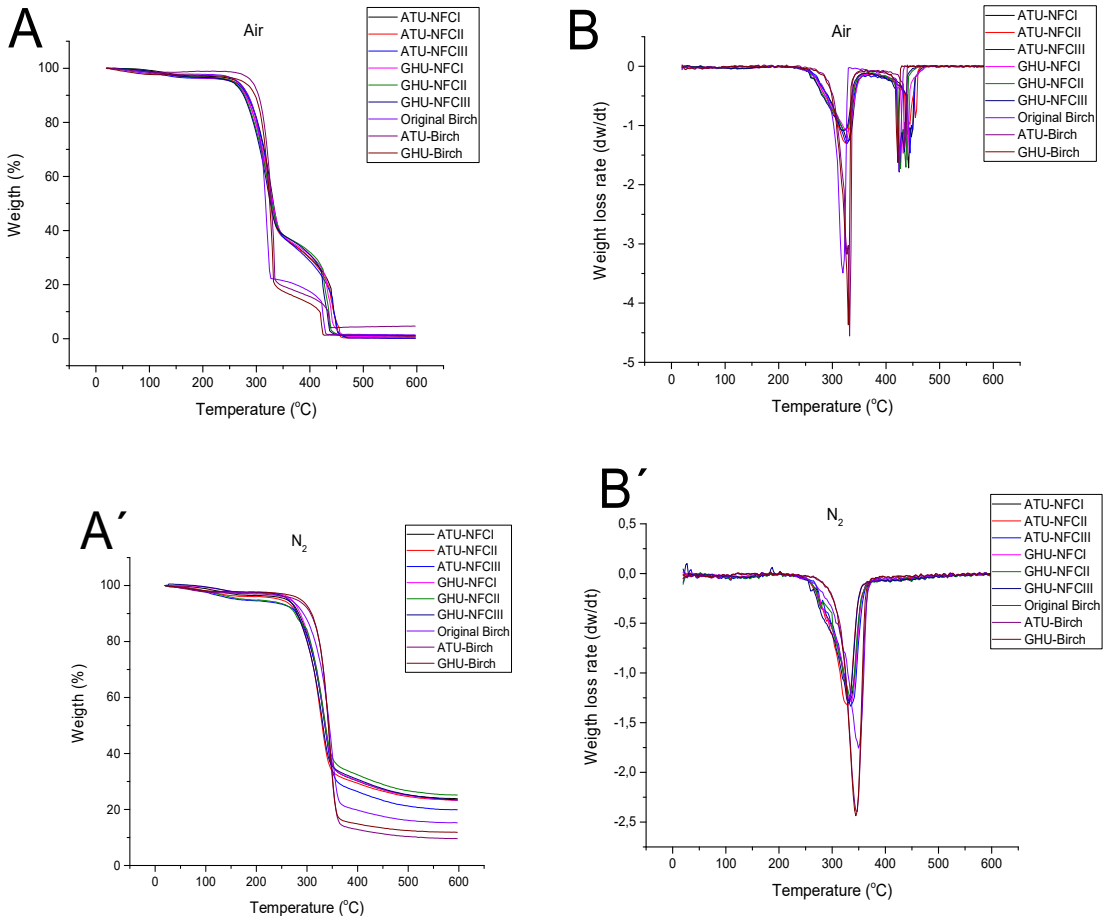

Figure 7. TGA curve of the samples at air (A) and N_2 (A´) condition, accordingly, with their first derivate curves of the TGA (DTG) at air (B) and N_2 (B´). (ATU = ammonium thiocyanate – urea DES; GHU = guanidine hydrochloride – urea DES; NFC = nanofibrillated cellulose; Birch = hardwood cellulose fiber).

Mechanical Characteristics of Nanofibril Films. The ultimate strengths prior to the specimens were entirely fractured are shown in Figure 8. Generally, all of the nanofibril films achieved good tensile strength (image A in Figure 8) ranging from approximately 135 to 189 MPa which is similar to periodate-based nanocellulose films (130–163 MPa)[49] and is much higher than multiple enzyme-pretreated NFC films (60–120 MPa).[50] The elastic modulus (image B in Figure 8) ranged from 6.4 to 7.7 GPa, which is comparable with films made previously of TEMPO-oxidized cellulose nanofibers (6–7 GPa)[51] and also similar to other solvent-cast NFC films (6 ± 1 GPa).[52] The films pretreated by ATU were, in most cases, more uniform and had higher strength properties compared to GHU films. ATU treated fibrils showed no linear dependency between processing severity and product strength (i.e., from I → II → III) while GHU-derived film strength was clearly deteriorated by continued processing. Similar decreasing trend was observed for film strain, but the degree of

microfluidization had quite a small impact on Young's modulus. The more uniform structure of ATU nanofibril films was also proved with FESEM images and the existence of the white flakes and clear porous regions in GHU nanofibril films may have weakened its properties (Figure 5).

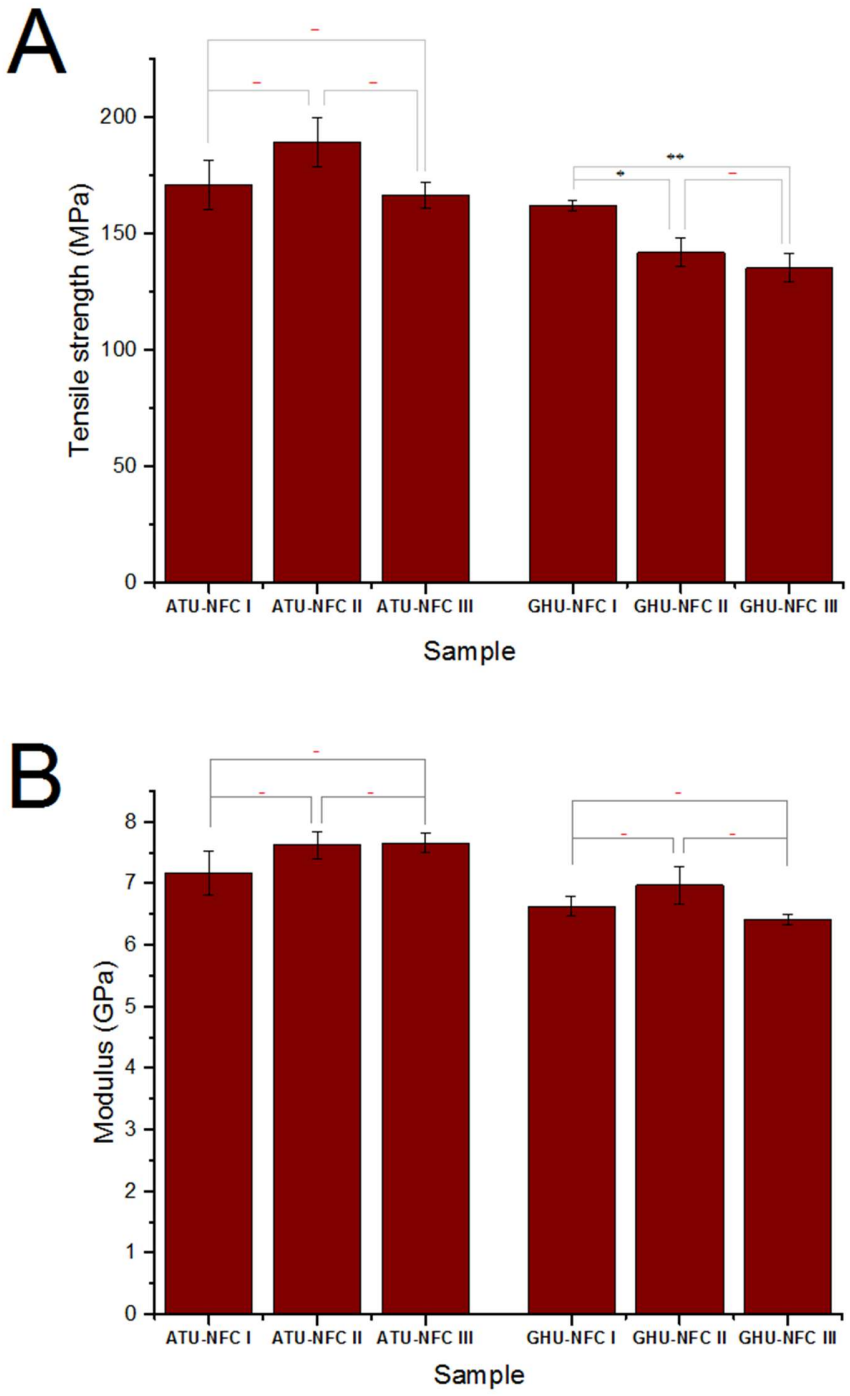

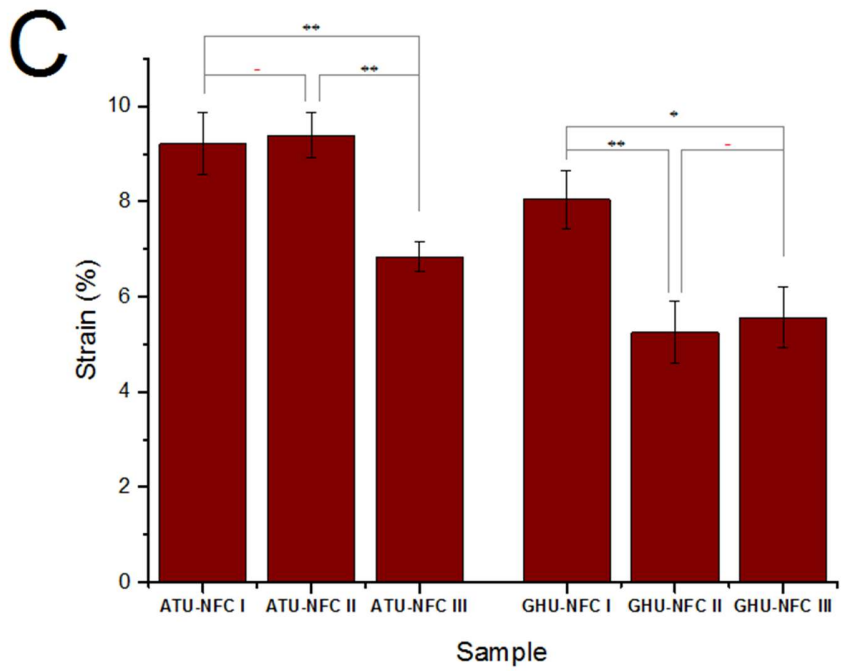

Figure 8. Tensile strength (A), Young's modulus (B), and strain (C) of nanofibril films. Data presented as mean ± standard error and analyzed using a one-way ANOVA, (*) $p<0.05$; (**) $p < 0.01$; (–) with no statistical significance.

Clear differences between the levels of mechanical treatments were seen especially with the DES of guanidine hydrochloride – urea. The increase in severity of nanofibrillation decreased the tensile strength of samples (image A in Figure 8). Beside the possible damages caused by guanidine hydrochloride pretreatment, the extended mechanical treatment may have reduced the strength of individual nanofibrils. In addition, the nanofibril films achieved notably higher strain values (5.3–9.4%) than previous oxygen barrier nanofibril films pretreated by oxidation approach (0.7–1.6%),[49] and also higher than NFC−talc films (approximately 5%).[43] However, the film elongation at the break had a decreasing trend with increased severity of microfluidization (image C in Figure 8). Hence, it is necessary to explore the optimum conditions for the disintegration of cellulose fibers from not only mechanical processes such as injection pressures, chamber sizes, and shapes point-of-view but also considering chemical pretreatment solvents such as the ratios and species in a DES, the synthesis temperature, and duration.

CONCLUSIONS

The ammonium thiocyanate – urea- and guanidine hydrochloride – urea- based DES systems were successfully applied as pretreatments for cellulose nanofibril production. Both DESs promoted the cellulose structure, loosening as indicated by an increase in fiber lateral dimension, while the DP of cellulose remained at the initial level after DES treatments. The cellulose nanofibril suspensions were slightly turbid and gel-like and passed through the microfluidizer smoothly without chamber clogging. Nanofibril films cast from nanofibril suspension achieved good mechanical properties and thermal stability. Generally, DES synthesized by ammonium thiocyanate and urea was more effective than the guanidine hydrochloride in terms of a higher DP and better swelling capacity for cellulose fiber, and a better mechanical property of the nanofibril films. DES -based systems are sustainable, easy to prepare, and relatively inexpensive, indicating green approaches for nanocellulose production, whereas DES properties and especially their forming mechanisms deserve further study to optimize the pretreatment methods for cellulose fiber nanofibrillation.

ASSOCIATED CONTENT

Supporting Information

The Supporting Information is available free of charge on the ACS Publications website at DOI: 10.1021/acsami.6b13625

TEM images with larger magnifications to observe the diameter and some details of the nanofibrils (PDF).

AUTHOR INFORMATION

Corresponding Author

*E-mail: Henrikki.Liimatainen@oulu.fi

ORCID: Henrikki Liimatainen 0000-0002-7911-2632

Author Contributions

The manuscript was written through contributions of all authors. All authors have given approval to the final version of the manuscript.

Notes

The authors declare no competing financial interest.

ACKNOWLEDGMENTS

The authors acknowledge Dr. Miikka Visanko for his expertise in mechanical strength measurement. Mr. Tommi Kokkonen is gratefully acknowledged for the thermogravimetric analysis. Dr. Ilkka Miinalainen is acknowledged for his help with the TEM and SEM images. We would like to also thank Mrs. Elisa Wirkkala for the limiting viscosity measurements.

REFERENCES

(1) Fanjul-Mosteirín, N.; Concellón, C.; del Amo, V. L-Isoleucine in a Choline Chloride/Ethylene Glycol Deep Eutectic Solvent: A Reusable Reaction Kit for the Asymmetric Cross-Aldol Carboligation. *Org. Lett.* **2016**, *18* (17), 4266–4269.

(2) Wagle, D. V.; Zhao, H.; Baker, G. A. Deep Eutectic Solvents: Sustainable Media for Nanoscale and Functional Materials. *Acc. Chem. Res.* **2014**, *47* (8), 2299–2308.

(3) Selkälä, T.; Sirviö, J. A.; Lorite, G. S.; Liimatainen, H. Anionically Stabilized Cellulose Nanofibrils through Succinylation Pretreatment in Urea–Lithium Chloride Deep Eutectic Solvent. *ChemSusChem* **2016**, *9* (21), 3074–3083.

(4) Ilgen, F.; Ott, D.; Kralisch, D.; Reil, C.; Palmberger, A.; König, B. Conversion of Carbohydrates into 5-Hydroxymethylfurfural in Highly Concentrated Low Melting Mixtures. *Green Chem.* **2009**, *11* (12), 1948.

(5) Yu, Y.; Lu, X.; Zhou, Q.; Dong, K.; Yao, H.; Zhang, S. Biodegradable Naphthenic Acid Ionic Liquids: Synthesis, Characterization, and Quantitative Structure-Biodegradation Relationship. *Chem. - Eur. J.* **2008**, *14* (35), 11174–11182.

(6) Singh, B.; Lobo, H.; Shankarling, G. Selective N-Alkylation of Aromatic Primary Amines Catalyzed by Bio-Catalyst or Deep Eutectic Solvent. *Catal. Lett.* **2011**, *141* (1), 178–182.

(7) Abbott, A. P.; Capper, G.; Gray, S. Design of Improved Deep Eutectic Solvents Using Hole Theory. *ChemPhysChem* **2006**, *7* (4), 803–806.

(8) Gu, C.; Tu, J. One-Step Fabrication of Nanostructured Ni Film with Lotus Effect from Deep Eutectic Solvent. *Langmuir* **2011**, *27* (16), 10132–10140.

(9) Gu, C.-D.; Zhang, J.-L.; Bai, W.-Q.; Tong, Y.-Y.; Wang, X.-L.; Tu, J.-P. Electro-Brush Plating from Deep Eutectic Solvent: A Case of Nanocrystalline Ni Coatings with Superior Mechanical Property and Corrosion Resistance. *J. Electrochem. Soc.* **2015**, *162* (4), D159–D165.

(10) Liao, H.-G.; Jiang, Y.-X.; Zhou, Z.-Y.; Chen, S.-P.; Sun, S.-G. Shape-Controlled Synthesis of Gold Nanoparticles in Deep Eutectic Solvents for Studies of Structure–Functionality Relationships in Electrocatalysis. *Angew. Chem. Int. Ed.* **2008**, *47* (47), 9100–9103.

(11) Carriazo, D.; Serrano, M. C.; Gutiérrez, M. C.; Ferrer, M. L.; del Monte, F. Deep-Eutectic Solvents Playing Multiple Roles in the Synthesis of Polymers and Related Materials. *Chem. Soc. Rev.* **2012**, *41* (14), 4996.

(12) Ge, X.; Gu, C. D.; Lu, Y.; Wang, X. L.; Tu, J. P. A Versatile Protocol for the Ionothermal Synthesis of Nanostructured Nickel Compounds as Energy Storage Materials from a Choline Chloride-Based Ionic Liquid. *J. Mater. Chem. A* **2013**, *1* (43), 13454.

(13) Zhang, H.; Lu, Y.; Gu, C.-D.; Wang, X.-L.; Tu, J.-P. Ionothermal Synthesis and Lithium Storage Performance of Core/shell Structured Amorphous@crystalline Ni–P Nanoparticles. *CrystEngComm* **2012**, *14* (23), 7942–7950.

(14) Xia, S.; Baker, G. A.; Li, H.; Ravula, S.; Zhao, H. Aqueous Ionic Liquids and Deep Eutectic Solvents for Cellulosic Biomass Pretreatment and Saccharification. *RSC Adv.* **2014**, *4* (21), 10586.

(15) Gunny, A. A. N.; Arbain, D.; Nashef, E. M.; Jamal, P. Applicability Evaluation of Deep Eutectic Solvents–Cellulase System for Lignocellulose Hydrolysis. *Bioresour. Technol.* **2015**, *181*, 297–302.

(16) Crawford, D. E.; Wright, L. A.; James, S. L.; Abbott, A. P. Efficient Continuous Synthesis of High Purity Deep Eutectic Solvents by Twin Screw Extrusion. *Chem. Commun.* **2016**, *52* (22), 4215–4218.
(17) Habibi, Y.; Lucia, L. A.; Rojas, O. J. Cellulose Nanocrystals: Chemistry, Self-Assembly, and Applications. *Chem. Rev.* **2010**, *110* (6), 3479–3500.
(18) Klemm, D.; Kramer, F.; Moritz, S.; Lindström, T.; Ankerfors, M.; Gray, D.; Dorris, A. Nanocelluloses: A New Family of Nature-Based Materials. *Angew. Chem. Int. Ed.* **2011**, *50* (24), 5438–5466.
(19) Mohieldin, S. D.; Zainudin, E. S.; Paridah, M. T.; Ainun, Z. M. Nanotechnology in Pulp and Paper Industries: A Review. *Key Eng. Mater.* **2011**, *471–472*, 251–256.
(20) Oksman, K.; Mathew, A. P.; Bondeson, D.; Kvien, I. Manufacturing Process of Cellulose Whiskers/polylactic Acid Nanocomposites. *Compos. Sci. Technol.* **2006**, *66* (15), 2776–2784.
(21) Sorrentino, A.; Gorrasi, G.; Vittoria, V. Potential Perspectives of Bio-Nanocomposites for Food Packaging Applications. *Trends Food Sci. Technol.* **2007**, *18* (2), 84–95.
(22) Ahola, S.; Österberg, M.; Laine, J. Cellulose Nanofibrils—adsorption with Poly(amideamine) Epichlorohydrin Studied by QCM-D and Application as a Paper Strength Additive. *Cellulose* **2008**, *15* (2), 303–314.
(23) Nakagaito, A. N.; Yano, H. Novel High-Strength Biocomposites Based on Microfibrillated Cellulose Having Nano-Order-Unit Web-like Network Structure. *Appl. Phys. A* **2005**, *80* (1), 155–159.
(24) Iwamoto, S.; Nakagaito, A. N.; Yano, H.; Nogi, M. Optically Transparent Composites Reinforced with Plant Fiber-Based Nanofibers. *Appl. Phys. A* **2005**, *81* (6), 1109–1112.
(25) Aulin, C.; Gällstedt, M.; Lindström, T. Oxygen and Oil Barrier Properties of Microfibrillated Cellulose Films and Coatings. *Cellulose* **2010**, *17* (3), 559–574.
(26) Herrick, F. W.; Casebier, R. L.; Hamilton, J. K.; Sandberg, K. R. Microfibrillated Cellulose: Morphology and Accessibility. *J Appl Polym Sci Appl Polym Symp U. S.* **1983**, *37*, 797–813.
(27) Siró, I.; Plackett, D. Microfibrillated Cellulose and New Nanocomposite Materials: A Review. *Cellulose* **2010**, *17* (3), 459–494.
(28) Saito, T.; Nishiyama, Y.; Putaux, J.-L.; Vignon, M.; Isogai, A. Homogeneous Suspensions of Individualized Microfibrils from TEMPO-Catalyzed Oxidation of Native Cellulose. *Biomacromolecules* **2006**, *7* (6), 1687–1691.
(29) Liimatainen, H.; Visanko, M.; Sirviö, J. A.; Hormi, O. E. O.; Niinimaki, J. Enhancement of the Nanofibrillation of Wood Cellulose through Sequential Periodate-Chlorite Oxidation. *Biomacromolecules* **2012**, *13* (5), 1592–1597.
(30) Henriksson, M.; Henriksson, G.; Berglund, L. A.; Lindström, T. An Environmentally Friendly Method for Enzyme-Assisted Preparation of Microfibrillated Cellulose (MFC) Nanofibers. *Eur. Polym. J.* **2007**, *43* (8), 3434–3441.
(31) Pedersen, M.; Meyer, A. S. Lignocellulose Pretreatment Severity - Relating pH to Biomatrix Opening. *New Biotechnol.* **2010**, *27* (6), 739–750.
(32) Lee, H. V.; Hamid, S. B. A.; Zain, S. K. Conversion of Lignocellulosic Biomass to Nanocellulose: Structure and Chemical Process. *Sci. World J.* **2014**, *2014*, 1–20.
(33) Sirviö, J. A.; Visanko, M.; Liimatainen, H. Deep Eutectic Solvent System Based on Choline Chloride-Urea as a Pre-Treatment for Nanofibrillation of Wood Cellulose. *Green Chem* **2015**, *17* (6), 3401–3406.

(34) Sirviö, J. A.; Visanko, M.; Liimatainen, H. Acidic Deep Eutectic Solvents As Hydrolytic Media for Cellulose Nanocrystal Production. *Biomacromolecules* **2016**, *17* (9), 3025–3032.
(35) Liimatainen, H.; Sirviö, J.; Haapala, A.; Hormi, O.; Niinimäki, J. Characterization of Highly Accessible Cellulose Microfibers Generated by Wet Stirred Media Milling. *Carbohydr. Polym.* **2011**, *83* (4), 2005–2010.
(36) Da Silva Perez, D.; Van Heiningen, A. R. P. Determination of Cellulose Degree of Polymerization in Chemical Pulps by Viscosimetry. *SEVENTH Eur. Workshop Lignocellul. PULP EWLP Proc.* **2002**, 393–396.
(37) Liimatainen, H.; Sirviö, J.; Haapala, A.; Hormi, O.; Niinimäki, J. Characterization of Highly Accessible Cellulose Microfibers Generated by Wet Stirred Media Milling. *Carbohydr. Polym.* **2011**, *83* (4), 2005–2010.
(38) Marsich, L.; Bonifacio, A.; Mandal, S.; Krol, S.; Beleites, C.; Sergo, V. Poly-L-Lysine-Coated Silver Nanoparticles as Positively Charged Substrates for Surface-Enhanced Raman Scattering. *Langmuir* **2012**, *28* (37), 13166–13171.
(39) Ray, D.; Sarkar, B. K. Characterization of Alkali-Treated Jute Fibers for Physical and Mechanical Properties. *J. Appl. Polym. Sci.* **2001**, *80* (7), 1013–1020.
(40) Siqueira, G.; Tapin-Lingua, S.; Bras, J.; da Silva Perez, D.; Dufresne, A. Morphological Investigation of Nanoparticles Obtained from Combined Mechanical Shearing, and Enzymatic and Acid Hydrolysis of Sisal Fibers. *Cellulose* **2010**, *17* (6), 1147–1158.
(41) Saito, T.; Kimura, S.; Nishiyama, Y.; Isogai, A. Cellulose Nanofibers Prepared by TEMPO-Mediated Oxidation of Native Cellulose. *Biomacromolecules* **2007**, *8* (8), 2485–2491.
(42) Saito, T.; Hirota, M.; Tamura, N.; Kimura, S.; Fukuzumi, H.; Heux, L.; Isogai, A. Individualization of Nano-Sized Plant Cellulose Fibrils by Direct Surface Carboxylation Using TEMPO Catalyst under Neutral Conditions. *Biomacromolecules* **2009**, *10* (7), 1992–1996.
(43) Liimatainen, H.; Ezekiel, N.; Sliz, R.; Ohenoja, K.; Sirviö, J. A.; Berglund, L.; Hormi, O.; Niinimäki, J. High-Strength Nanocellulose–Talc Hybrid Barrier Films. *ACS Appl. Mater. Interfaces* **2013**, *5* (24), 13412–13418.
(44) Nam, S.; Condon, B. D.; Foston, M. B.; Chang, S. Enhanced Thermal and Combustion Resistance of Cotton Linked to Natural Inorganic Salt Components. *Cellulose* **2013**, *21* (1), 791–802.
(45) Poletto, M.; Zattera, A. J.; Santana, R. M. C. Structural Differences between Wood Species: Evidence from Chemical Composition, FTIR Spectroscopy, and Thermogravimetric Analysis. *J. Appl. Polym. Sci.* **2012**, *126* (S1), E337–E344.
(46) Deng, J.; Xiong, T.; Wang, H.; Zheng, A.; Wang, Y. Effects of Cellulose, Hemicellulose, and Lignin on the Structure and Morphology of Porous Carbons. *ACS Sustain. Chem. Eng.* **2016**, *4* (7), 3750–3756.
(47) Li, J.; Wei, X.; Wang, Q.; Chen, J.; Chang, G.; Kong, L.; Su, J.; Liu, Y. Homogeneous Isolation of Nanocellulose from Sugarcane Bagasse by High Pressure Homogenization. *Carbohydr. Polym.* **2012**, *90* (4), 1609–1613.
(48) Dhar, P.; Bhardwaj, U.; Kumar, A.; Katiyar, V. Cellulose Nanocrystals: A Potential Nanofiller for Food Packaging Applications. In *Food Additives and Packaging*; ACS Symposium Series; American Chemical Society, 2014; Vol. 1162, pp 197–239.
(49) Sirviö, J. A.; Kolehmainen, A.; Visanko, M.; Liimatainen, H.; Niinimäki, J.; Hormi, O. E. O. Strong, Self-Standing Oxygen Barrier Films from Nanocelluloses Modified with

Regioselective Oxidative Treatments. *ACS Appl. Mater. Interfaces* **2014**, *6* (16), 14384–14390.
(50) Qing, Y.; Sabo, R.; Wu, Y.; Zhu, J. Y.; Cai, Z. Self-Assembled Optically Transparent Cellulose Nanofibril Films: Effect of Nanofibril Morphology and Drying Procedure. *Cellulose* **2015**, *22* (2), 1091–1102.
(51) Isogai, A.; Saito, T.; Fukuzumi, H. TEMPO-Oxidized Cellulose Nanofibers. *Nanoscale* **2011**, *3* (1), 71–85.
(52) Cranston, E. D.; Eita, M.; Johansson, E.; Netrval, J.; Salajková, M.; Arwin, H.; Wågberg, L. Determination of Young's Modulus for Nanofibrillated Cellulose Multilayer Thin Films Using Buckling Mechanics. *Biomacromolecules* **2011**, *12* (4), 961–969.

Abstract Graphic

Deep eutectic solvent-pretreatment for cellulose fibers

Mechanical disintegrated nanofibrils